# Positive Span of Force and Torque Components in Three Dimensional Four Finger Force Closure Grasps

Nattee Niparnan        Attawith Sudsang        Prabhas Chongstitvatana

*Department of Computer Engineering, Faculty of Engineering, Chulalongkorn University, Bangkok, THAILAND*

*{nattee,attawith}@cp.eng.chula.ac.th, Prabhas.C@chula.ac.th*

## Abstract

Testing whether a given grasp achieves force closure is a fundamental problem in grasping. Unfortunately, most of the force closure testing methods avoid dealing with the true quadratic friction cones by resorting to some linear approximation which unavoidably sacrifices completeness and accuracy. This paper presents a method, considering the true nonlinear friction cone, that can be used as a filter that quickly reject non force closure grasps. The method is based on a necessary condition stating that a force closure grasp must be able to generate wrenches that positively span the force space and the torque space separately. The geometric relationship between the friction cones and the corresponding force space and torque space is analyzed to help construct an efficient test of the condition. Due to the superior speed of the test over a complete method, the overall performance improvement is paramount. In our experiment, speed up factor of 20 or greater can be achieved when testing a large number of grasps on various test objects.

## 1   INTRODUCTION

Grasping has been an active research area in robotics since the pioneering works of Salisbury and Roth [1, 2]. Recommended survey can be found in [3, 4]. Shared amongst all grasping problems is one central question: whether an object can be *securely grasped*. It is widely accepted that a secure grasp must be able to resist any external disturbance. The term *force closure* is introduced to represent such property. Apparently, synthesis of force closure grasps emerges naturally as one of the most dominant problems in grasping (see [5] for a past survey). Another topic of equal importance is the grasp analysis problem: given a grasp, determine its quality. Since all grasp synthesis methods require their results to satisfy particular properties such as force closure, grasp analysis is essentially a key into the grasp synthesis problem. Grasp synthesis and grasp analysis are intrinsically related.

While typical grasp synthesis frameworks rely on tightly integrating and embedding grasp analysis methods, some recently proposed grasp synthesis approaches rely on separable grasp analysis method explicitly. This new trend, which further emphasizes the role of grasp analysis, has become an attractive choice for the grasp synthesis problems in which the grasped object is modeled by discrete representation of its boundary such as point cloud

or discretized curves (see [6, 7, 8, 9] for some examples). This representation naturally serves the real-world grasping applications in which the object model is not provided in advance and has to be acquired through some sensory devices. The underlying idea is to systematically search for an optimal grasping configuration in the finite space of such representation such that each candidate configuration is tested for desirability by a grasp analysis method. Different methods under this scheme vary by applying different search policy. A method based on hill climbing or branch and bound search is presented in [10, 11]. Other optimizers are also adopted such as evolutionary computation as in [12, 13], or generate-and-test approach as in [14]. Unlike traditional grasp synthesis framework, this search based framework can conveniently take into account any grasp analysis method. By developing a matching grasp analysis method, the user can compute a grasp that meets the requirement of their grasping task at hand without having to derive from scratch a new grasp synthesis method for the particular requirement. This advantage however arrives with the cost for assessing every candidate grasp by the grasp analysis method. To maximize the benefit of this scheme, the grasp analysis method needs to be computationally efficient.

This work focuses on improving the computational efficiency of a grasp analysis method. We consider a grasp analysis approach called *filtering approach* [14]. A typical approach measures a grasp according to one particular grasp analysis method. However, the filtering approach employs two-level analysis. At the first level, a grasp is analyzed using a relatively fast method that tests for the necessity of force closure property of the grasp. If the grasp does not pass the necessity imposed in the first level, the grasp is rejected. Since the first level imposes only the necessity, not the sufficiency, of the force closure property, the method used in the first level can be computed efficiently. The first level method sacrifices completeness in favor of fast rejection of non force closure grasps. If a grasp passes all necessary requirements, the grasp is then passed to the second level where a grasp is tested with a typical grasp analysis method that completely analyzes the quality of the grasp. In other words, the first level acts as a *filter* that permit only necessary grasps to be tested with the second level.

The filtering approach is especially beneficial in the situation where there are several grasps to be considered and a large portion of them are non force closure grasps. This is because some non force closure grasps will be detected in the first level and rejected efficiently. Obviously, a force closure grasp is tested by both the first level method and the second level method. Hence, the filtering approach should not be used when most grasps being considered are force closure grasp. The search based scheme mentioned earlier, which we believe to become the new standard practice in grasp synthesis, is a particular situation where filtering approach could excel. Interestingly, branch and bound technique itself could be considered as a filtering approach that is applied on a macro level. For example, see the work of Watanabe and Yoshikawa [11] where a relaxed condition which can be computed faster are used as a relaxed heuristic to prune unnecessary candidates from being evaluated by a more time consuming method. Another favorable situation for the filtering approach is when all force closure grasps are to be computed from the object [15, 16, 17, 18, 19, 9].

An interesting and pervasive issue in force closure testing is the nonlinearity of the representation of friction cones. Unfortunately, majority of force closure tests do not directly deal with the issue but choose to avoid this hindrance by introducing linearity into the problem at the cost of some noticeable incompleteness. See for example the condition of $\theta$-positively span in [20, 21] or several conditions based on the linearization of the

friction model [22, 23]. It is the work of Han *et al.* [24] that tackles this nonlinearity problem directly. The work, based on the research of Buss *et al.* [25], formulates the friction constraints as linear matrix inequalities (LMIs) and transforms the problem into a convex optimization problem. This method is complete, i.e., it considers directly the quadratic friction cone without linearization. However, it comes with the cost of efficiency since convex optimization takes considerable amount of computation power.

In this paper, we propose a novel necessary condition of force closure and its efficient implementation. The condition can be used as a first level method for the filtering approach. The condition, geometrically derived from the nonlinear friction model, can be computed very efficiently. It is based on the fact that a force closure grasp must be able to exert wrenches that positively span the force space and the torque space independently (the reverse is not necessarily true). The geometry that relates friction cones to the force and torque components is analyzed so that an efficient algorithm for testing the condition can be constructed. The condition can be evaluated much faster (e.g., by using our proposed algorithm) than existing force closure tests that handle the nonlinear friction cones directly. In our experiments in which large number of grasps on various objects are tested, the performance improvement by this filtering approach compared with using a complete test alone is paramount. In some cases, speed-up factor of 20 or greater can be achieved. The performance advantage is indeed desirable to the search based scheme in which many queries need to be made.

The rest of the paper is organized as follows. Section 2 briefly describes past background of grasping introducing our condition of force closure. In Section 3, we describe the key idea of our method which consists of two separated conditions. Each condition is described in Section 4 and Section 5. In Section 7 we present numerical examples comparing efficiency gained by our approach. Finally, Section 8 concludes our work.

## 2   GRASPING BACKGROUND

A grasp is described by a set of contact points. A grasp is said to achieve force closure when the grasp is able to counter any external disturbance to the grasped object. Interaction with the object is represented by forces and torques. To represent a force and a torque simultaneously, a force $\boldsymbol{f} = (f_x, f_y, f_z)$ and a torque $\boldsymbol{\tau} = (\tau_x, \tau_y, \tau_z)$ are combined into an entity called *wrench* $\boldsymbol{w} = (f_x, f_y, f_z, \tau_x, \tau_y, \tau_z) \in \mathbb{R}^6$.

This work assumes hard contact with Coulomb friction model [26]. As opposed to a soft contact, a hard contact is unable to exert a pure torque. A torque from a contact must be the result of the applied force only. As a result, a contact point at $\boldsymbol{p}$ that exerts a force $\boldsymbol{f}$ can be represented by a wrench $\boldsymbol{w} = (\boldsymbol{f}, \boldsymbol{p} \times \boldsymbol{f})$. Coulomb friction model indicates that a contact point can exert some tangential force without slippage. The maximum ratio between the magnitude of tangential force and the magnitude of the force in the normal direction is indicated by the frictional coefficient $\mu$ between the object and the contact point of the grasping finger. In other words, the net force exerted by a non-slipping contact must lie in a cone at the contact point whose axis lies in the normal direction and its half angle [1] is given by $\theta = \tan^{-1}(\mu)$. This force cone is referred to as *friction cone*. It is shown in [27] that a force closure grasp with four hard contact points is possible for any 3D object. It is assumed in this work that the number of contact points is limited to four and the frictional coefficient at any contact points are the

---

[1] the angle between the normal and the vector on the boundary of the cone

same.

We associate each contact point with a set of wrenches exertable by the contact point. A grasp is said to achieve force closure when its contact points are able to produce any wrench in the wrench space $\mathbb{R}^6$. Canonically, the force closure property considers only the direction of wrenches while the magnitude is neglected. A set of wrenches are said to achieve force closure when their positive linear combination can produce a wrench in every direction in the space. The term $\mathbb{R}^n$-*positive span* is reserved to represent such property.

**Definition 2.1** *A set of $n$ wrenches $\{\boldsymbol{w}_1, \ldots, \boldsymbol{w}_n\}$ positively spans $\mathbb{R}^n$ if and only if, for any vector $\boldsymbol{v}$ in $\mathbb{R}^n$, there exists nonnegative constants $\alpha_1, \ldots, \alpha_n$ such that $\boldsymbol{v} = \alpha_1 \boldsymbol{w}_1 + \ldots + \alpha_n \boldsymbol{w}_n$.*

## 2.1 Preliminaries and Notations

We denote by $\mathrm{int}(\cdot)$ and $\mathrm{ri}(\cdot)$ the interior and the relative interior[2], respectively. Let $P$ be an arbitrary plane through the origin in $\mathbb{R}^3$. The plane $P$ can be described by its normal vector $\boldsymbol{n}$. Formally, $P = \{\boldsymbol{x} | \boldsymbol{x} \cdot \boldsymbol{n} = 0\}$. We say that a vector $\boldsymbol{x}$ is on the positive (resp. negative) side of $P$ when the sign of $\boldsymbol{x} \cdot \boldsymbol{n}$ is positive (resp. negative). Two vectors are said to be on different sides of $P$ when one of them is on the positive side and the other is on the negative side.

In the upcoming section, we will need to describe the set of all positive combinations of vectors. For this purpose, let us refer to the set of all positive combinations of all vectors in a vector set $W$ (i.e., $\{\sum \alpha_i \boldsymbol{v}_i | \alpha_i \geq 0, \boldsymbol{v}_i \in W\}$) as a *positive span* of $W$. Also, let the positive span of $W$ be denoted by $\Psi(W)$. When $W$ does not positively span $\mathbb{R}^n$, $\Psi(W)$ forms a convex subspace that can be represented by the intersection of several half spaces each of which is defined by a plane tangent to $\Psi(W)$. Each plane is called a *bounding plane*. The normal vector of a bounding plane is assumed to point inward $\Psi(W)$.

# 3 NECESSARY CONDITION FOR FOUR FINGER FORCE CLOSURE GRASP

In this section, we present a new necessary condition of force closure for a four finger grasp. Our condition is based on the following proposition regarding the property of a positive span.

**Proposition 3.1** *A necessary condition for a set of vectors to positively span $\mathbb{R}^n$ is that the projection of the vectors on any subspace $\mathbb{R}^{k<n}$ must positively span the subspace.*

It is clear that the condition is necessary but not sufficient. Figure 1 illustrates some examples that satisfy Proposition 3.1. Our condition is the application of the proposition on the wrench space. The wrench space consists of two distinct subspaces: the force space and the torque space, each is $\mathbb{R}^3$. Our condition checks whether the set of wrenches associated with the contact points positively span the force space and positively span

---

[2]A relative interior of a set is the interior relative to the affine hull of the set. Intuitively speaking, a relative interior are all points not on the relative edge of the set, e.g., A relative interior of a line segment is the segment minus its endpoints, regardless of the dimension where the line is situated.
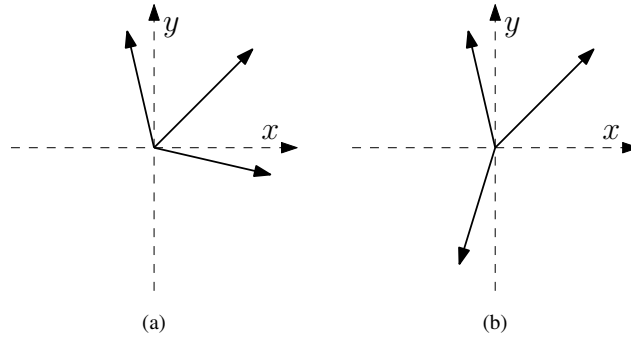
(a)                    (b)

Figure 1: Example of vectors that satisfied Proposition 3.1. (a) the vectors do not positively span the space. (b) the vectors positively span the space.
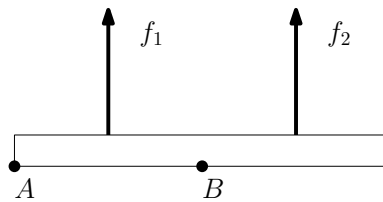


Figure 2: Example of forces.

the torque space. When the wrenches fail to positively span the force space or the torque space, the wrenches definitely fail to achieve force closure.

It should be noted that any subspace can be used in Proposition 3.1. However, a larger subspace usually has a higher chance to catch more non force closure grasps. This fact emphasizes preference to high dimensional subspace. Nevertheless, for the condition to be useful, it must also be computationally inexpensive. The force space and the torque space each describes an entity whose structure can be exploited. This allows us to derive an efficient computational implementation.

Asserting whether the force space is positively spanned is straightforward. It amounts to testing whether the corresponding force cones of the contact points positively span the force space. Positively spanning of the torque space is, however, more complicated to test. A torque varies according to the choice of the origin, although the force closure property as a whole is invariant to the relocation of the origin. It is possible that for some choice of the origin, a non force closure grasp may have its wrenches positively span the torque space. See for example the planar case in Figure 2. In the figure, it is clear that the contact points generate only counterclockwise torques when the origin is located at $A$. However, when the origin is located at $B$, the contact points generate both clockwise and counterclockwise torques, thus positively span the torque space. The effect of this situation can be reduced by considering whether the torque space is positively spanned with respect to various choices of the origin of the workspace. A higher number of origin considered, a higher chance that we can detect a non force closure grasp from the projection of its wrenches on the torque space.

It should be observed that when the choice of the origin is made such that the origin is located at a contact point, that contact point produces no torque. Thus, there are one less torque set to be taken into consideration

when compared to a general choice of the origin.

## 3.1 The Proposed Condition

Based on the aforementioned discussion, we propose a novel necessary condition for force closure as follows. We consider two subspaces: the force space and the torque space. For the torque space, four choices of the origin are to be determined, each is the contact point of the grasp being considered. This results in the total of five tests: one considers the force space and the other four consider the torque space. Let the contact point be located at $p_1, \ldots, p_4$ and let $F_i$ and $T_i$ be the set of forces and the set of torques associated with the contact point at $p_i$, Our five tests are listed as follows.

1. $F_1, \ldots, F_4$ must positively span the force space.

2. Let the origin be located at $p_1$; $T_2, T_3, T_4$ must positively span the torque space.

3. Let the origin be located at $p_2$; $T_1, T_3, T_4$ must positively span the torque space.

4. Let the origin be located at $p_3$; $T_1, T_2, T_4$ must positively span the torque space.

5. Let the origin be located at $p_4$; $T_1, T_2, T_3$ must positively span the torque space.

The detail of the test of the force space and the torque space are discussed in Section 4 and Section 5, respectively.

In the actual implementation, the test is performed sequentially starting from the test of force space and then proceeds to each of torque space. As soon as any test fails, it is guaranteed that the grasp does not achieve force closure.

It should also be emphasized that the condition given in this section is a necessary condition. The condition does not completely checking force closure grasp. Rather, it is used in a filtering approach to identify a non force closure grasp with small computational effort.

## 3.2 Preliminaries for positively spanning in $\mathbb{R}^3$

Both the torque space and the force space are $\mathbb{R}^3$ subspace. It has been shown in [28] that at least four vectors are needed to positively span $\mathbb{R}^3$. The following proposition describes a necessary and sufficient condition for four vectors to positively span $\mathbb{R}^3$.

**Proposition 3.2** *Four vectors $w_1, \ldots, w_4$ positively span $\mathbb{R}^3$ when the negative of any of these vectors lies inside the relative interior of the pyramid formed by the other three vectors.*

Ding *et al.* provided a proof of Proposition 3.2 which can be found in [29].

Proposition 3.2 indicates that if there exists at least one vector that its negative lies inside the cone formed by the other three, the four vectors positively span $\mathbb{R}^3$. It also implies that if at least one vector has its negative *not* lying strictly inside the cone, we can immediately conclude that they do not positively span $\mathbb{R}^3$. Following this

implication, the next proposition provides a simple condition for a set of vectors to not positively span the $\mathbb{R}^3$ space.

**Proposition 3.3** *Let $W$ be a set of vectors. If there exists a plane $P$ through the origin such that every vector in $W$ lies either on $P$ or on the same side of $P$, then $W$ does not positively span $\mathbb{R}^3$.*

# 4 $\mathbb{R}^3$-POSITIVE SPAN OF FORCE COMPONENTS

This section introduces a method to test whether four 3D friction cones positively span $\mathbb{R}^3$. Since positively spanning property concerns only directions of vectors, it is sufficient to represent a cone by its axis, which is the inward normal vector of the contact point, and its half angle.

Let us denote by $\boldsymbol{n}_i$ and $\mu$ the unit inward normal of contact point $\boldsymbol{p}_i$ and the respective friction coefficient. The half angle of the friction cone of $\boldsymbol{p}_i$ is $\theta = \tan(\mu)$. The frictional coefficient is assumed to be the same for all contact points. In other words, $F_i = \{\boldsymbol{f}|(\boldsymbol{f} \cdot \boldsymbol{n}_i)/|\boldsymbol{f}| \geq \cos\theta\}$. We also define a negative cone $-F_i = \{-\boldsymbol{f}|\boldsymbol{f} \in F_i\}$ to be the cone consisting of the negative of all members of $F_i$. The following lemma describes a necessary and sufficient condition for several force cones to positively span $\mathbb{R}^3$. The condition is essentially an extension of Proposition 3.2.

**Lemma 4.1** *Let $F_1, \ldots, F_n$ be force cones of contact points at $\boldsymbol{p}_1, \ldots, \boldsymbol{p}_n$. These force cones positively span $\mathbb{R}^3$ if and only if there exists an intersection between the interior of the negative of any cone and the interior of the positive span of the other three cones.*

*Proof.* Let $\mathcal{W} = \Psi(\bigcup_{i=2}^n F_i)$. Assume that $\text{int}(-F_1) \cap \text{int}(\mathcal{W})$ is not empty. Let $\boldsymbol{v}$ be an arbitrary vector in the intersection. Since $\boldsymbol{v}$ is a member of the interior of $\mathcal{W}$, we can always find three non-coplanar vectors $\boldsymbol{w}_1, \boldsymbol{w}_2, \boldsymbol{w}_3$ in $\mathcal{W}$ such that $\boldsymbol{v}$ lies in the interior of the pyramid formed by these three vectors. Since $\boldsymbol{v}$ is the negative of $-\boldsymbol{v}$ which is a vector in $F_1$, Proposition 3.2 can be applied to deduce that $\boldsymbol{w}_1, \boldsymbol{w}_2, \boldsymbol{w}_3$ and $\boldsymbol{v}$ positively span $\mathbb{R}^3$. The condition is therefore sufficient.

To prove that the condition is necessary, we will show that if $\text{int}(-F_1) \cap \text{int}(\mathcal{W}) = \emptyset$, no vector in $-\mathcal{W}$ can be written as a positive combination of members of $F_1, \ldots, F_n$ (therefore they do not positively span $\mathbb{R}^3$). Let us assume oppositely that some vector in $-\mathcal{W}$ can be written as a positive combination of a vector $\boldsymbol{a} \in F_1$ and some vector in $\mathcal{W}$. Since $\text{int}(-F_1) \cap \text{int}(\mathcal{W}) = \emptyset$, $-\boldsymbol{a}$ does not lie in $\mathcal{W}$. This implies that there exists a bounding plane $P$ of $\mathcal{W}$ such that $-\boldsymbol{a}$ is on the negative side of $P$. In other words, $\boldsymbol{a}$ lies on the positive side of $P$. Obviously, any vector in $-\mathcal{W}$ is on the negative side of $P$. Hence, it is not possible to write any vector in $-\mathcal{W}$ as a positive combination of $\boldsymbol{a}$ and some vector in $\mathcal{W}$. A contradiction results which indicates that the condition is necessary. $\square$

To test whether four friction cones positively span $\mathbb{R}^3$, we pick two arbitrary cones, says $F_1$ and $F_2$, and then check whether these two cones positively span $\mathbb{R}^3$. If they do not, we pick another cone, says $F_3$. From Lemma 4.1, the only possibility that these three cones positively span $\mathbb{R}^3$ is that $\text{int}(-F_3) \cap \Psi(F_1 \cup F_2) \neq \emptyset$. Thus, we check for such intersection. If none such intersection exists, we take the last cone ($F_4$) into account. Again, by

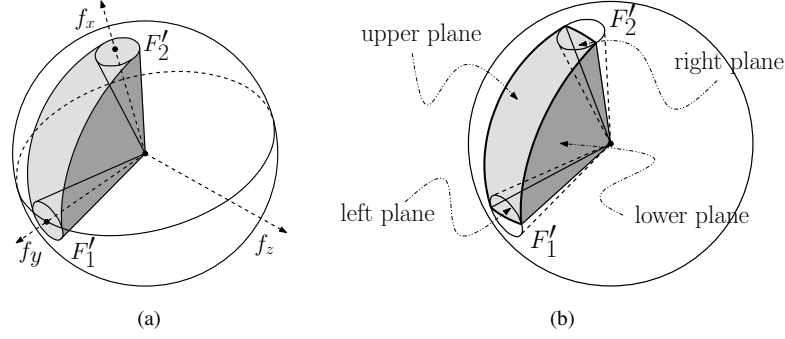(a)                                              (b)

Figure 3: Two force cones and a unit sphere. (a) The shaded area represents the intersection between the positive span of two cones and the sphere. (b) The inner region containing the area $\Psi(F_1' \cup F_2')) - \text{int}(F_2') - \text{int}(F_2')$

.

Lemma 4.1, we know that these four cones positively span $\mathbb{R}^3$ only when $\text{int}(-F_4) \cap \Psi(F_1 \cup F_2 \cup F_3) \neq \emptyset$. The method to test whether a negative cone intersects with the positive span of one cone, two cones and three cones are described in Section 4.1, 4.2 and 4.3, respectively.

## 4.1 Two Force Cones Positively Spanning $\mathbb{R}^3$

Let the two force cones be $F_1$ and $F_2$ (recall that these cones have their apex at the origin of the force space). From Lemma 4.1, two force cones positively span $\mathbb{R}^3$ only when there exists an intersection between the interior of one cone and the negative of the other cone. Two cones intersect when the angle between their axes is smaller than the sum of their half angles. Hence, to test whether $F_1$ and $F_2$ positively span $\mathbb{R}^3$, it is to be asserted whether the angle between $\boldsymbol{n}_1$ and $-\boldsymbol{n}_2$ is smaller than $2\theta$.

## 4.2 Three Force Cones Positively Spanning $\mathbb{R}^3$

Let the three force cones be $F_1, \ldots, F_3$. Let us assume that two of them, namely $F_1$ and $F_2$, do not positively span $\mathbb{R}^3$. From Lemma 4.1, to test if $F_1, \ldots, F_3$ positively span $\mathbb{R}^3$, it has to be asserted whether $\text{int}(-F_3)$ intersects $\text{int}(\Psi(F_1 \cup F_2))$. Observe that the condition is the same as asserting whether the vector $-\boldsymbol{n}_3$ intersects $\text{int}(\Psi(F_1' \cup F_2'))$, where $F_i'$ is the cone $F_i$ whose half angle is increased by $\theta$.

Since the condition concerns only the direction of force cones, let us represent a force cone by its intersection with a unit sphere. On the surface of the sphere, the intersection of $\Psi(F_1 \cup F_2)$ resembles a racetrack (see Figure 3a). Figure 4 displays the transformation.

When a vector $-\boldsymbol{n}_3$ intersects $\text{int}(\Psi(F_1' \cup F_2'))$, it must lie in one of the following areas: 1) $\text{int}(F_1')$, 2) $\text{int}(F_2')$, and 3) the area in between $F_1'$ and $F_2'$. The method tests whether $-\boldsymbol{n}_3$ lies in one of these areas. Each of the first two areas is simply a circular cone. The vector $-\boldsymbol{n}_3$ lies in the interior of a circular cone only when the angle between $-\boldsymbol{n}_3$ and the axis of the cone is smaller than the cone's half angle. The in-between area is the
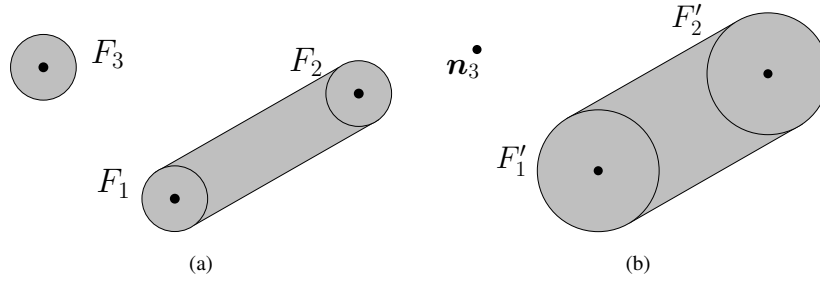
Figure 4: Force cones as seen on the surface of the unit sphere. The picture does not preserve linearity. (a) $F_3$ and $\Psi(F_1 \cup F_2)$. (b) Enlarging of $F_1$ and $F_2$ by $\theta$.

remaining area $(\operatorname{int}(\Psi(F_1' \cup F_2')) - \operatorname{int}(F_1') - \operatorname{int}(F_2'))$. Instead of considering this area, we consider a four sided pyramid which is a super set of the in-between area and is a subset of $\operatorname{int}(\Psi(F_1' \cup F_2'))$. The pyramid, shown in Figure 3b, is bounded by four planes through the origin: two of which are the planes that are tangent to both $F_1'$ and $F_2'$ (see Figure 5a). We call these planes the upper and the lower planes. Each of the other two bounding planes is associated with each force cone. For each cone, we construct a bounding plane that contains the two tangent vectors at which the upper and the lower planes touch the cone. These two bounding planes are called the left plane and the right plane (also see Figure 5b).

Let $P$ be the plane containing $\boldsymbol{n}_1$ and $\boldsymbol{n}_2$. Let $\boldsymbol{r}_i$ be the vector lying in $P$ that is perpendicular to $\boldsymbol{n}_i$. We restrict $\boldsymbol{r}_1$ to point toward $\boldsymbol{n}_2$ and $\boldsymbol{r}_2$ to point toward $\boldsymbol{n}_1$, i.e., $\boldsymbol{r}_1 \cdot \boldsymbol{n}_2 > 0$ and $\boldsymbol{r}_2 \cdot \boldsymbol{n}_1 > 0$. Obviously, $\boldsymbol{r}_1$ and $\boldsymbol{r}_2$ are the normal vectors of the left and the right plane, respectively (see Figure 6a). The vectors at the intersection between the left (resp. right) plane and $F_1'$ (resp. $F_2'$) are the vectors that also lie on the upper and lower plane. Let $\boldsymbol{t}_{1a}$ and $\boldsymbol{t}_{1b}$ (resp. $\boldsymbol{t}_{2a}$ and $\boldsymbol{t}_{2b}$) be such vectors. The vectors $\boldsymbol{t}_{1a}$ and $\boldsymbol{t}_{1b}$ (resp. $\boldsymbol{t}_{2a}$ and $\boldsymbol{t}_{2b}$) can be calculated by rotating $\boldsymbol{n}_1$ (resp. $\boldsymbol{n}_2$) around $\boldsymbol{r}_1$ (resp. $\boldsymbol{r}_2$) by $-2\theta$ and $2\theta$, respectively (see Figure 6b). The normal vectors of the upper plane and the lower plane are $\boldsymbol{t}_{2b} \times \boldsymbol{t}_{1a}$ and $\boldsymbol{t}_{1b} \times \boldsymbol{t}_{2a}$, respectively. With the normal vectors, testing whether $-\boldsymbol{n}_3$ lies inside the pyramid is simply testing the dot products between $-\boldsymbol{n}_3$ and the normal vectors.

## 4.3 Four Force Cones Positively Spanning $\mathbb{R}^3$

Let the four force cones be $F_1, \ldots, F_4$. Let us assume that three of them, namely $F_1, F_2$ and $F_3$, do not positively span $\mathbb{R}^3$. It has to be asserted whether $\operatorname{int}(-F_4)$ intersects $\operatorname{int}(\Psi(F_1 \cup F_2 \cup F_3))$. Analogous to the previous cases, it is to be asserted whether $-\boldsymbol{n}_4$ intersects $\mathcal{W}' = \operatorname{int}(\Psi(F_1' \cup F_2' \cup F_3'))$. Figure 7 illustrates $\mathcal{W}'$ as observed on the surface of the sphere. Obviously, $-\boldsymbol{n}_4$ is inside $\mathcal{W}'$ when either it is inside $\operatorname{int}(\Psi(F_1' \cup F_2'))$, inside $\operatorname{int}(\Psi(F_2' \cup F_3'))$, or inside $\operatorname{int}(\Psi(F_3' \cup F_1'))$, or, finally, inside the pyramid defined by the axes of the three cones. The last area is illustrated as the shaded region in Figure 7. The method described in Section 4.2 can be employed to check the first three containments.

The intersection between $-\boldsymbol{n}_4$ and the pyramidal area can be tested by considering the dot products between $-\boldsymbol{n}_4$ and the inward normal vectors of the facets of the pyramid. The normal vectors of the three facets are ordered pairwise cross products of $\boldsymbol{n}_1$, $\boldsymbol{n}_2$ and $\boldsymbol{n}_3$. However, a correct order of $\boldsymbol{n}_1$, $\boldsymbol{n}_2$ and $\boldsymbol{n}_3$ has to be determined.
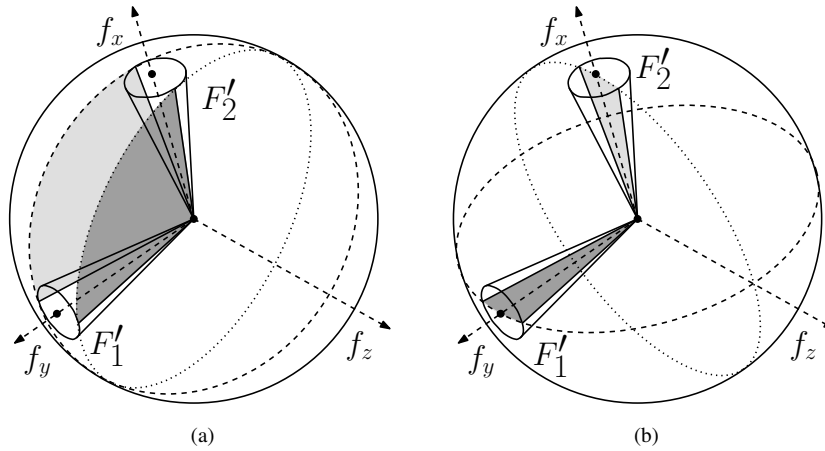
Figure 5: (a) The upper and lower plane, represented by the shaded area. The dashed line and the dotted line represent the great circles bounding the upper plane and the lower plane, respectively. The planes tangentially touch both cones. (b) The left and right plane, represented by the shaded area. The dashed line and the dotted line represent the great circles bounding the left plane and the right plane, respectively. The planes contain the double tangents of the same cone.
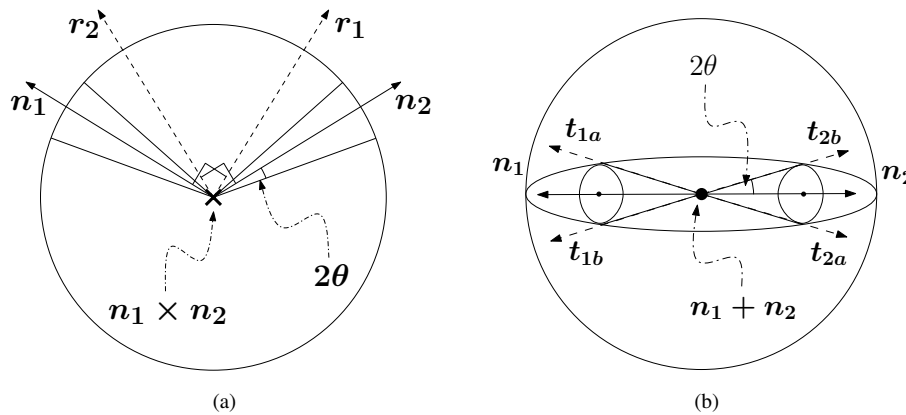


Figure 6: Computation of the planes bounding the pyramid. (a) The cone as viewed along $n_1 \times n_2$ which points into the page. The vectors $r_1$ and $r_2$ is the normal vector of the left and right plane. The vector $n_1, n_2, r_1$ and $r_2$ all lies on the same plane as the page. (b) The cones as viewed along $n_1 + n_2$ which points out from the page. The vector $t_{1a}$ and $t_{1b}$ are the double tangents of $F_1'$ which is computed by rotating $n_1$ around $r_1$ by $-2\theta$ and $2\theta$, respectively.
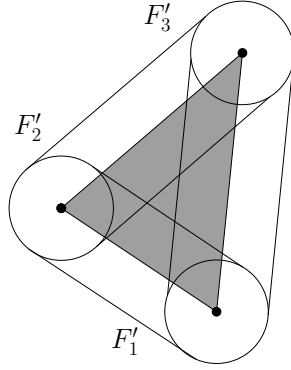
Figure 7: $\mathcal{W}'$ as seen on the surface of the sphere. The shaded region is the area need to be checked in addition to the other checking that can be done by the previous method.

There can be only two distinct orders, namely $(\boldsymbol{n}_1, \boldsymbol{n}_2, \boldsymbol{n}_3)$ or $(\boldsymbol{n}_2, \boldsymbol{n}_1, \boldsymbol{n}_3)$. The correct order can be obtained by considering the facet that contain $\boldsymbol{n}_1$ and $\boldsymbol{n}_2$. The normal vector of the facet that contains $\boldsymbol{n}_1$ and $\boldsymbol{n}_2$ is either 1) $\boldsymbol{n}_1 \times \boldsymbol{n}_2$, or 2) $\boldsymbol{n}_2 \times \boldsymbol{n}_1$. The correct direction is the one that has positive dot product with $\boldsymbol{n}_3$, because $\boldsymbol{n}_3$ must be on the positive side of the plane containing $\boldsymbol{n}_1$ and $\boldsymbol{n}_2$.

# 5 $\mathbb{R}^3$-POSITIVE SPAN OF TORQUE COMPONENTS

This section examines the geometric relationship between the torque space and the friction cones. Let us denote by $T_i$ the set of all torques generated by all forces in $F_i$ (which is the friction cone of $\boldsymbol{p}_i$), i.e., $T_i = \{\boldsymbol{p}_i \times \boldsymbol{f} | \boldsymbol{f} \in F_i\}$. Since any torque $\boldsymbol{p}_i \times \boldsymbol{f}$ is obviously perpendicular to $\boldsymbol{p}_i$, $T_i$ must lie on the plane through the origin and perpendicular to $\boldsymbol{p}_i$. Let us call this plane $P_i$.

   To describe how $T_i$ occupies $P_i$, let us consider a plane $P_f$ through the origin that contains $\boldsymbol{p}_i$ and intersects with $F_i$. Observe that a torque generated by any force in $P_f \cap F_i$ (a slice of $F_i$ on $P_f$) must lie in the direction parallel to the normal of $P_f$. The idea is to consider all possible planes $P_f$ so that all forces in $F_i$ can be taken into account (see Figure 8a). With this idea, it can be shown that $T_i$ lies on $P_i$ in two different ways: 1) $\boldsymbol{p}_i$ is not in $\text{int}(F_i)$. As the plane $P_f$ rotates around $\boldsymbol{p}_i$ and continuously sweeps through $F_i$, correspondingly generated torques continuously sweep $P_i$. As a result, the resulting torques, $T_i$, form a fan of torques, i.e., the set of all positive combinations of two boundary torques. 2) When $\boldsymbol{p}_i$ is in $\text{int}(F_i)$, $T_i$ covers the entire plane $P_i$. This is the case because for each possible $P_f$, resulting torques span two opposite directions on $P_i$. Since $P_f$ in this case intersects with $F_i$ in all orientations around $\boldsymbol{p}_i$, resulting torques cover all directions in $P_i$.

   To compute the resulting fan of case 1, it is necessary to identify the two boundary torques of the fan. Since each of these torques is generated when $P_f$ touches $F_i$, let us describe how to compute the corresponding forces $\boldsymbol{f}_a, \boldsymbol{f}_b \in F_i$ at which this event occurs. Let $\Pi$ be the plane lying perpendicular to $\boldsymbol{n}_i$ at the distance $\boldsymbol{p}_i \cdot \boldsymbol{n}_i$ from the origin. Consider the intersection of $\Pi$ with $F_i$ and the lines through the vectors $\boldsymbol{n}_i, \boldsymbol{p}_i, \boldsymbol{f}_a, \boldsymbol{f}_b$. Figure 8b illustrates this intersection as observed on $\Pi$. From the figure, $\boldsymbol{f}_a$ and $\boldsymbol{f}_b$ can be determined from the angle $\phi$. Let

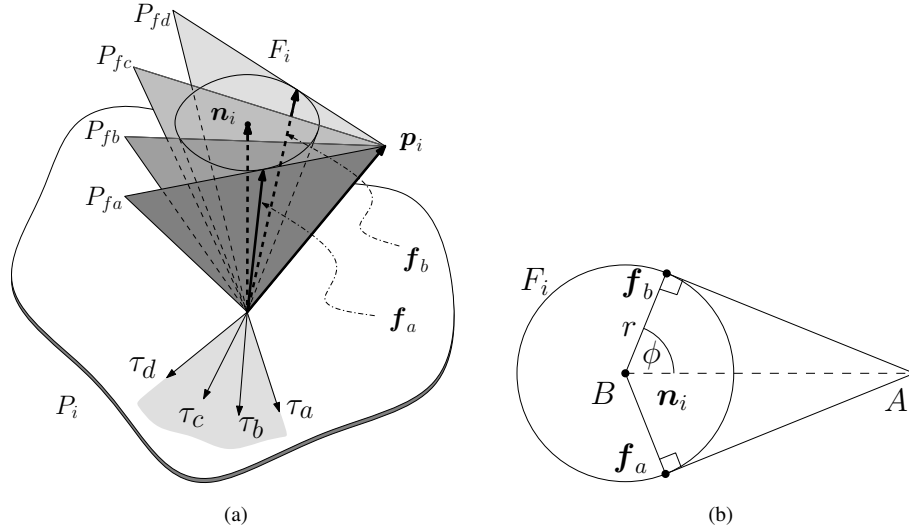Figure 8: (a) A force cone $F_i$ and its position vector $\boldsymbol{p}_i$. The curved line represents plane $P_i$ which is perpendicular to $\boldsymbol{p}_i$. The plane $P_{fa}, \ldots, P_{fd}$ are planes through the origin that contains $\boldsymbol{p}_i$ and intersects $F_i$. $P_{fa}$ and $P_{fd}$ tangentially touch $F_i$ and the intersection of which is $\boldsymbol{f}_a$ and $\boldsymbol{f}_b$, respectively. Vector $\tau_a, \ldots, \tau_d$ represents the direction of torque generated from $P_{fa}, \ldots, P_{fd}$, respectively. (b) The plane $\Pi$, lying perpendicular to $\boldsymbol{n}_f$ at the distance $\boldsymbol{p}_i \cdot \boldsymbol{n}_i$ from the origin. The radius of the boundary of the cone is $r = \tan(\theta)(\boldsymbol{p}_i \cdot \boldsymbol{n}_f)$. The angle $\phi$ equals to $\arccos(r/|\overline{AB}|)$.

$A$ and $B$ be the intersection on $\Pi$ of the line through $\boldsymbol{p}_i$ and the line through $\boldsymbol{n}_i$, respectively. The angle $\phi$ is equal to $\arccos(r/|\overline{AB}|)$ where $r$ is the radius of the circle from the intersection of $F_i$ and $\Pi$, i.e., $r = \tan(\theta)(\boldsymbol{p}_i \cdot \boldsymbol{n}_i)$.

## 5.1 Three Torque Sets Positively Spanning $\mathbb{R}^3$

We have established that a torque set of any contact point is either a fan or a plane. The problem is to assert whether three torque sets positively span $\mathbb{R}^3$. When any of the torque sets forms a plane, these sets positively span $\mathbb{R}^3$ only when there exists vectors lying on different sides of this plane. Let $\boldsymbol{n}_t$ be the normal vector of the plane. If the other two sets are fans, we check whether the dot products between the boundary vectors of the fans and $\boldsymbol{n}_t$ have different signs. If the other sets are planes, we check whether the normal vectors of the other planes are not parallel to $\boldsymbol{n}_t$.

The remaining case is when all three torque sets are fans. This is done in the same manner as in the case of three force cones (Section 4.2). First, we check whether two of them, says $T_1$ and $T_2$, positively span $\mathbb{R}^3$. If not, we check whether the remaining fan, says $T_3$, and the positive span of $T_1$ and $T_2$ positively span $\mathbb{R}^3$.

A fan is a positive span of its boundary vectors. Checking whether two fans positively span $\mathbb{R}^3$ is equivalent to checking whether their boundary vectors positively span $\mathbb{R}^3$. There are four boundary vectors. By Proposition 3.2, the four vectors positively span $\mathbb{R}^3$ only when the negative of one of them lies inside the interior of the pyramid of the remaining three. The method for checking whether a vector lies inside a pyramid of three vectors,
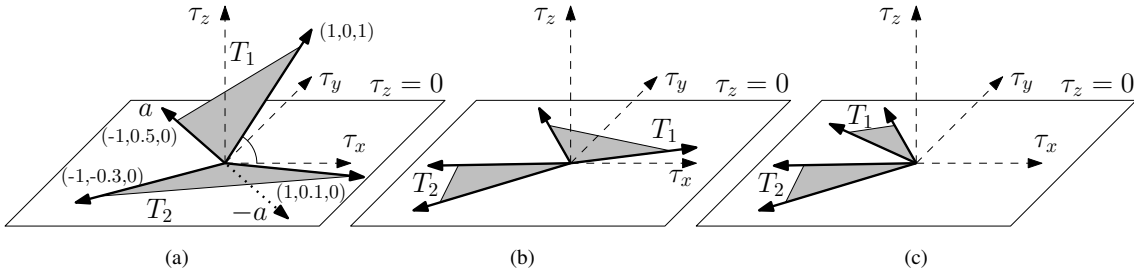
Figure 9: The two torque sets form a half space bounded by the plane $\tau_z = 0$. The plane in the figure represents the plane $\tau_z = 0$. The shaded regions represents $T_1$ and $T_2$. (a) The half space case. Notice that three boundary vectors lies on $\tau_z = 0$ and the vector $a$ being the boundary of $T_1$ has its negative lies inside $T_2$. (b) The plane case. (c) the fan case.

as described in the test of four force cone (Section 4.3), can be used directly.

Now, let us assume that $T_1$ and $T_2$ do not positively span $\mathbb{R}^3$. It is to be asserted whether $T_3$ and $\Psi(T_1 \cup T_2)$ positively span $\mathbb{R}^3$. Since $T_1$ and $T_2$ are fans, their positive span can only be a half space, a larger fan, a plane, or a pyramid. Each case is considered separately as follows.

### 5.1.1 The Half Space Case

This case can be detected by verifying that one fan, says $T_1$, has exactly one of its boundary vectors lying on the plane containing the other fan, says $T_2$, and the negative of that boundary vector lies strictly inside $T_2$ (see Figure 9a). In such case, the half space is defined by the plane $P_2$. The three fans positively span $\mathbb{R}^3$ only when at least one of the boundary vectors of $T_3$ lies outside the half space. This can be identified from the sign of the dot products of the boundary vectors of $T_3$ and the normal vector of $P_2$.

### 5.1.2 The Plane and Fan Cases

When both $T_1$ and $T_2$ lie on the same plane, their positive span forms either a fan or a plane (see Figure 9b and 9c). It is a plane when the boundary vectors of $T_1$ and $T_2$ positively span the plane. This case is identified by checking whether one fan has its negative boundary vectors lie inside the other fan, and vice versa. In this case, the three fans positively span $\mathbb{R}^3$ only when the two boundary vectors of $T_3$ lie on different sides of $P_1$. If $\Psi(T_1 \cup T_2)$ is a fan, we can check whether $\Psi(T_1 \cup T_2)$ and $T_3$ positively span $\mathbb{R}^3$ using the same method for the case of two fans.

### 5.1.3   The Pyramid Case

The only remaining case is that $\Psi(T_1 \cup T_2)$ is a pyramid. The next lemma describes a necessary and sufficient condition for the three fans to positively span $\mathbb{R}^3$ in this case.

**Lemma 5.1** *Let $T_1, T_2$ and $T_3$ be three fans and $\Psi(T_1 \cup T_2)$ forms a pyramid. These fans positively span $\mathbb{R}^3$ if and only if $-T_3$ intersects the interior of the pyramid.*

*Proof.*  To prove that the condition is sufficient, let $w$ be a member of the intersection between $-T_3$ and the interior of the pyramid. Since $w$ is in the interior of the pyramid, there always exist three non-coplanar vectors lying in the pyramid such that $w$ lies inside the interior of the cone formed by these three vectors. By Proposition 3.2, the three fans positively span $\mathbb{R}^3$.

To prove that the condition is necessary, it will be shown that the fans do not positively span $\mathbb{R}^3$ if $-T_3$ does not intersect the interior of the pyramid. A pyramid can be expressed by the intersection of several bounding half spaces $\mathcal{H}_1, \ldots, \mathcal{H}_l$. We assume that there is no vector in $-T_3$ that intersects with the interior of $\mathcal{W}$. Therefore, for each $w \in T_3$, there exists some $H_m, 1 \leq m \leq l$ that does not contain $-w$. This means that wrench $w$ and fans $T_1$ and $T_2$ must lie in the same half space $H_m$. This implies that $w$ and $T_1$ and $T_2$ do not positively span $\mathbb{R}^3$.

$\square$

A pyramid is represented by the intersection of a set of half spaces, each of which is described by a bounding plane containing the boundary torque vectors of $T_1$ and $T_2$. We represent the bounding planes of the pyramid by an ordered sequence of boundary torque vectors $S = (v_1, v_2, \ldots, v_l)$. Each bounding plane is a plane whose normal vector is the cross product of $v_i$ and $v_{i+1}$ (with the last facet being defined by $v_l \times v_1$). Let us denote by $\mathcal{T}$ the pyramid and by $B_1, \ldots, B_l$ the bounding facets of the pyramid. The fan $-T_3$ can intersect the interior of $\mathcal{T}$ in three possible cases: 1) $-T_3$ does not intersect with any $B_i$ but it lies in $\text{int}(\mathcal{T})$, 2) $-T_3$ intersects with $\text{ri}(B_i)$ for some $i$ such that $-T_3$ and $B_i$ do not lie on the same plane, and 3) $-T_3$ intersects with the common boundary vector of $B_i$ and $B_{i+1}$ when the other boundary vectors of $B_i$ and $B_{i+1}$ lie on different sides of the plane containing $-T_3$. Fig. 10 demonstrates examples of each case.

These three cases can be easily identified provided that the sequence $S$ is known. Case 1 can be detected by testing whether a vector in $\text{ri}(-T_3)$, says the middle vector of $T_3$, lies in the positive side of the bounding plane of the pyramid. This can be done easily by checking the sign of the dot product between the middle vector of $\text{ri}(-T_3)$ and the normal vector of the plane, which is $v_i \times v_{i+1}$. If all dot products are positive, the vectors lies inside the pyramid. For case 2, we enumerate every $B_i$ and test for its intersection with $-T_3$. This is the same as asking whether $B_i$ and $T_3$ positively span $\mathbb{R}^3$. Since $B_i$ is a fan, the same method for testing whether $T_1$ and $T_2$ positively span $\mathbb{R}^3$ can directly be used. Case 3 occurs when a boundary vector of $B_i$ lies on $\text{ri}(-T_3)$ and some part of $\text{ri}(-T_3)$ lies in $\text{int}(\mathcal{T})$. Let $-v_l^3$ and $-v_r^3$ denote the boundary vectors of $-T_3$. We can test whether an arbitrary vector $v$ lies on $\text{ri}(-T_3)$ by considering the cross product of $v$ and each boundary vector of $-T_3$, i.e., the vectors $v \times -v_l^3$ and $v \times -v_r^3$. If these two cross products lies on the same line but pointing into different
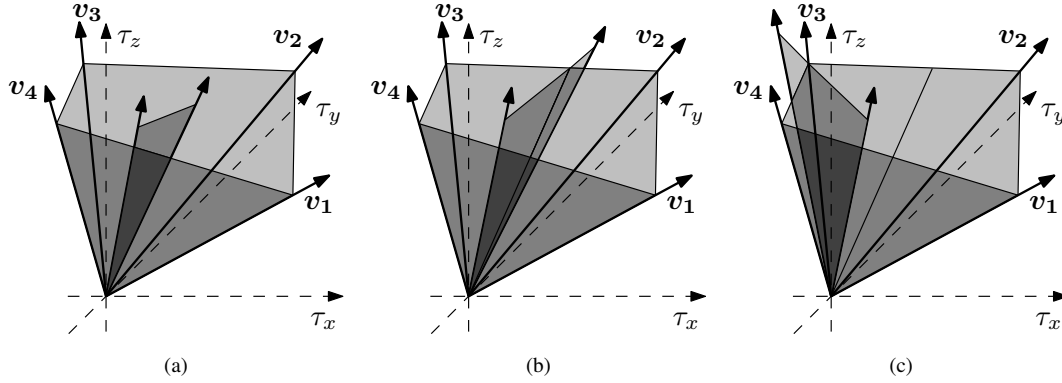
Figure 10: Example of intersection between $\mathrm{ri}(-T_3)$ and $\mathcal{T}$. (a) Case 1 (b) Case 2 (c) Case 3

directions and are not $\mathbf{0}$, $\boldsymbol{v}$ lies inside $\mathrm{ri}(-T_3)$. Assume that $\boldsymbol{v}_i$ lies on $\mathrm{ri}(-T_3)$, it is to be asserted that $\boldsymbol{v}_{i-1}$ and $\boldsymbol{v}_{i+1}$ lie on different sides of the plane through $-T_3$.

The tests of these three cases all rely on a query for determining which side of a given plane a vector lies on. A dot product between the vector and the normal vector of the plane can be used for this query. The remaining problem is the computation of $S$. It is to be determined which boundary torque vectors constitute the sequence and in which order. Such sequence can be shifted freely, i.e., the sequences $(\boldsymbol{v}_1, \boldsymbol{v}_2, \boldsymbol{v}_3, \boldsymbol{v}_4)$, $(\boldsymbol{v}_2, \boldsymbol{v}_3, \boldsymbol{v}_4, \boldsymbol{v}_1)$ and $(\boldsymbol{v}_4, \boldsymbol{v}_1, \boldsymbol{v}_2, \boldsymbol{v}_3)$ represent the same pyramid.

Notice that computation of $S$ which represents a 3D convex hull *is similar to the computation of a 2D convex hull of four points*. The pyramid is a 3D convex hull described by a sequence of vectors. A pair of adjacent vectors determines a plane such that the other vectors in the sequence lie on the same side of the plane. For the case of the 2D convex hull of four points, the convex hull is described by a sequence of points. A pair of adjacent points determines a line such that the other points in the sequence lie on the same side of the line. Analogy exists on the requirement of the bounding entities. The difference is that: in the case of a pyramid, the bounding entities are 3D vectors while in the case of a 2D convex hull, the bounding entities are 2D points.

From this observation, a method that computes a 2D convex hull can be used to compute the pyramid, given that the method relies only on an operation that determines the side of a bounding entity, e.g., the side of a vector with respect to a facet of a convex hull. The gift wrapping algorithm or Graham's Scan can be easily modified to perform the task. Nevertheless, we instead propose a more efficient method tailored specifically to compute a convex hull of four vectors. The method is described in detail in Section 5.2.

## 5.2 Computing the Convex Hull of Four Vectors

Let the four vectors be arbitrarily denoted by $\boldsymbol{p}_1, \boldsymbol{p}_2, \boldsymbol{q}_1$ and $\boldsymbol{q}_2$ and let us define $P$ as a fan bounded by $\boldsymbol{p}_1$ and $\boldsymbol{p}_2$ and also define $Q$ as a fan bounded by $\boldsymbol{q}_1$ and $\boldsymbol{q}_2$. The underlying idea of our convex hull algorithm comes from observing how $P$ and $Q$ lie with respect to each other.

To characterize how fans $P$ and $Q$ lie with respect to each other, let us define $t_i^p = \mathrm{sgn}((\boldsymbol{p}_1 \times \boldsymbol{p}_2) \cdot \boldsymbol{q}_i), i = 1, 2$, and $t_i^q = \mathrm{sgn}((\boldsymbol{q}_1 \times \boldsymbol{q}_2) \cdot \boldsymbol{p}_i), i = 1, 2$, where $\mathrm{sgn}(x)$ is $-1, 0$ or $+1$ when $x$ is respectively negative, zero or

positive, respectively. From the definition, $t_i^p$ (resp. $t_i^q$) takes on the value of $0, +1$ or $-1$ when $\boldsymbol{q}_i$ (resp. $\boldsymbol{p}_i$) is exactly on, on the positive or on the negative side of the plane containing the fan $P$ (resp. fan $Q$). With this setting, arrangement of fans $P$ and $Q$ can be classified into one of the following three cases.

### 5.2.1   When $t_1^p = t_2^p$ and $t_1^q = t_2^q$

This case is illustrated in Fig. 11a. For simplicity, the figure is presented in the context of 2D convex hull where a point and a segment are analogous to a vector and a fan in our case. Side of a point with respect to the line that contains a segment is analogous to side of a vector with respect to the plane that contains a fan.

Obviously, the resulting convex hull is a concatenation of the boundary vectors of fans $P$ and $Q$, i.e., $(\boldsymbol{p}_k, \boldsymbol{p}_l, \boldsymbol{q}_m, \boldsymbol{q}_n)$ where $k \neq l, m \neq n$ and $k, l, m, n \in \{1, 2\}$. Assignment of $k, l, m$ and $n$ has to be made such that $(\boldsymbol{p}_k, \boldsymbol{p}_l, \boldsymbol{q}_m, \boldsymbol{q}_n)$ is in the counterclockwise order. It is easy to verify that this requirement can be satisfied by the following rule: When $t_1^q = t_2^q = +1$, we set $k = 1$ and $l = 2$, otherwise we set $k = 2$ and $l = 1$, and when $t_1^p = t_2^p = +1$, we set $m = 1$ and $n = 2$, otherwise we set $m = 2$ and $n = 1$.

It should be noted that it is not possible for $t_1^p = t_2^p = 0$ or $t_1^q = t_2^q = $ to be happen in this case. This is because $t_1^p = t_2^p = 0$ implies that $\boldsymbol{p}_1$ and $\boldsymbol{p}_2$ lies on the same plane as $Q$, hence they do not form a pyramid.

### 5.2.2   When $t_1^p \neq t_2^p$ and $t_1^q \neq t_2^q$

An example of this case is shown in Fig. 11b. Since the condition indicates that fans $P$ and $Q$ cross each other, the resulting convex hull is an interwoven sequence of the vectors from the two fans, i.e., $(\boldsymbol{p}_1, \boldsymbol{q}_m, \boldsymbol{p}_2, \boldsymbol{q}_n)$ where $m \neq n$ and $m, n \in \{1, 2\}$. Assignment of $m$ and $n$ need to cause the sequence to follow the counterclockwise order. This requires $m$ and $n$ to be chosen such that $t_m^p = -1$ *or* $t_n^p = +1$ (either $t_m^p$ or $t_n^p$ is allowed to be zero in case of three coplanar vectors; see Fig. 11c for example).

### 5.2.3   When $t_1^p = t_2^p$ and $t_1^q \neq t_2^q$, or when $t_1^p \neq t_2^p$ and $t_1^q = t_2^q$

As illustrated in Fig. 11d, the resulting convex hull consists of only three vectors; one vector is discarded. Let us describe only the case in which $t_1^p = t_2^p$ and $t_1^q \neq t_2^q$ (the other case is treated likewise). In this case, either $\boldsymbol{q}_1$ or $\boldsymbol{q}_2$ (not both) has to be discarded because it lies inside the convex hull. If $\boldsymbol{q}_1$ and $\boldsymbol{q}_2$ are on the positive side of fan $P$ ($t_1^p = t_2^p = +1$), the convex hull can be written in the form $(\boldsymbol{p}_1, \boldsymbol{p}_2, \boldsymbol{q}_m), m \in \{1, 2\}$. When no three vectors are coplanar, it is easy to verify that the value of $m$ must be chosen such that $t_m^q = -1$. However, when some three vectors are coplanar, it is possible that $t_1^q \neq -1$ and $t_2^q \neq -1$. When this occurs, choose $m$ such that $t_m^q = 0$ in order to correctly eliminate the redundant vector. For the case that $\boldsymbol{q}_1$ and $\boldsymbol{q}_2$ are on the negative side of fan $P$, we will have the resulting convex hull $(\boldsymbol{p}_2, \boldsymbol{p}_1, \boldsymbol{q}_m)$ where the value of $m$ must be chosen such that $t_m^q = +1$ if possible, otherwise choose $m$ such that $t_m^q = 0$.
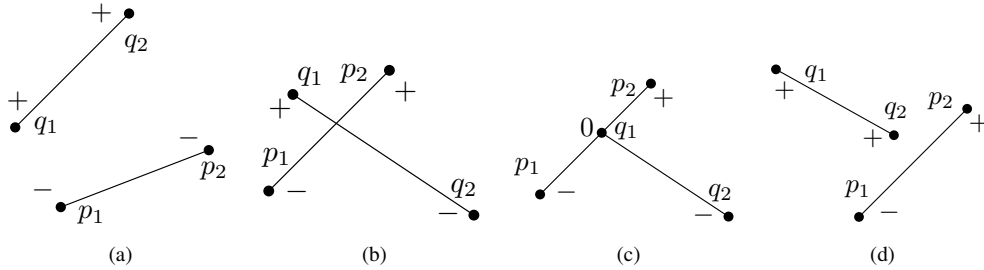
Figure 11: Arrangements of two segments forming a convex hull. The sign $+$ and $-$ indicates the value of $t_i^p$ and $t_i^q$. The plus sign $(+)$ indicates that the point is on the left of the other segment while the minus sign means that the point is on the right.

# 6  COMPUTATIONAL COMPLEXITY ANALYSIS

Our proposed condition is designed specifically for four finger grasp. Since the input size (the number of fingers) is fixed, asymptotic complexity analysis (which describes the growth of the running time as a function of input size) is irrelevant. To describe the computational complexity of our test in a somewhat more implementation independent than actual running time, we count the number of geometric operations of 3D vectors on which our test heavily relies.

For testing whether the force space is positively spanned, the proposed algorithm consists of three specific methods for the case of two cones, three cones and four cones. Majority of the operations performed by each method are cross products, dot products and rotations of a vector. Vector rotation is done by multiplication of a rotation matrix and a vector which is equivalent to three dot products. From counting, the entire operation uses at most 85 equivalent dot products and 11 cross products.

For the torque components, our algorithm requires four queries of positively spanning in the torque space, each of which is done with respect to a different origin. Each query requires a calculation of three torque fans, a testing whether two torque fans positively span the torque space and finally, a testing whether three torque fans positively span the torque space. For the case with three torque fans, the worst case scenario is when two of the fans form a pyramid and the negative of the remaining fan does not intersect any bounding facet causing the method to check the first two cases as described in Section 5.1.3. In this worst case, a single query requires 25 equivalent dot products and 27 cross products.

# 7  NUMERICAL EXAMPLE

The presented condition and implementation are introduced as a necessary condition which guarantees that a grasp not satisfying the condition does not achieve force closure while the force closure property of a grasp satisfying the condition is undetermined. An additional complete method is therefore needed to test these satisfying grasps. We will refer to a grasp satisfying the condition that actually is not a force closure grasp as a *false positive*. Our condition sacrifices completeness in favor of an efficiency in rejection. To benefit from the condition, the
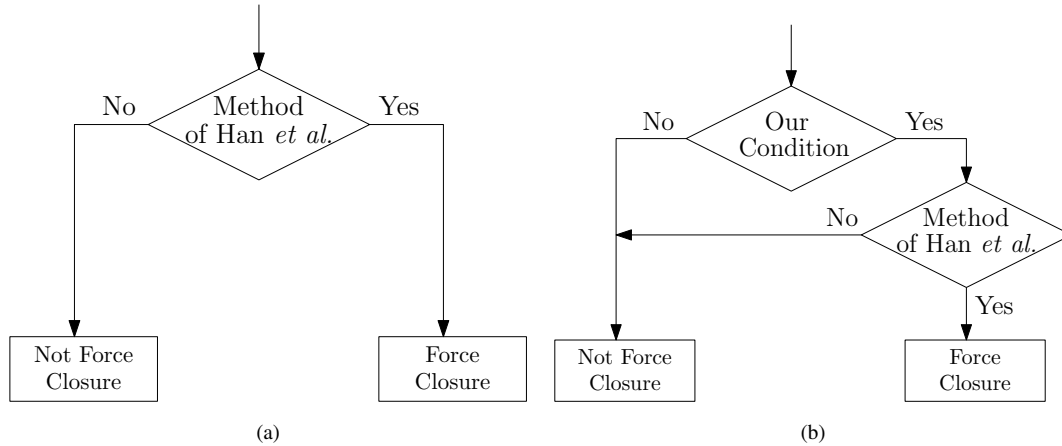
Figure 12: Flowchart of force closure testing method. (a) The method of Han *et al.* (b)The method of Han *et al.* with our condition as a filtering criteria.

time additionally taken by our condition in the case of false positive must be offset by the time saved from the reduced number of performed complete methods.

To help justify the benefit of our approach, we compare two grasp analysis frameworks: a canonical framework which uses a complete method to assert force closure and our filtering approach which uses the same complete method together with the presented condition as a filtering criteria. We select a complete test for force closure presented by Han *et al.* [24] for comparison. The method in [24] is selected because it considers directly the quadratic friction cone without linearization, yielding most theoretical accuracy. Figure 12 illustrates the flowchart of both methods.

## 7.1 Method for Force Closure Test by Han *et al.* [24]

Briefly speaking, the method of Han *et al.* formulate the problem as an *LMI feasibility problem*. A grasping configuration and the wrenches exerted by each contact is described by a vector $x = \{x_{11}, x_{12}, \ldots, x_{ij}, \ldots, x_{nm}\}$ and a mapping matrix $G$. The component $x_{ij}$ of vector $x \in \mathbb{R}^{mn}$ indicates the magnitude of j$^{th}$ component of intensity vector at i$^{th}$ contact point where $n$ and $m$ indicates the number of contact point and the number of components of intensity vectors, respectively.

Let us consider a grasp with two hard frictional contacts for an example. A hard contact with friction can be described by a force it exerts. The exerting force can be described by three components: one for the magnitude of the normal direction and the other two for the force vector in the tangential direction. Hence, this grasp can be described by a vector $x = \{x_{11}, x_{12}, x_{13}, x_{21}, x_{22}, x_{23}\}$ where $x_{i1}$ is the magnitude of the force in the normal direction of the $i^{th}$ contact and $x_{i2}$, $x_{i3}$ are the magnitude of the tangential force of $i^{th}$ contact.

The matrix $G \in \mathbb{R}^{6 \times mn}$ transforms $x$ into a net wrench which is $Gx$. A nontrivial solution to $Gx = 0$ indicates an equilibrium grasp. We let $V$ be a matrix whose columns are basis vectors of the null space of $G$. Hence, an equilibrium grasp can be written as $x = Vz$ where $z$ is a free variable.

Based on the work of Buss *et al.* [25], the Coulomb Friction model can be represented in the form of LMI as $P(\boldsymbol{x}) \succeq 0$ where $\succeq 0$ denotes semi-positive definiteness. When the inequality is written as positive definite condition, i.e., $P(\boldsymbol{x}) \succ 0$, the force is restricted to lies in the interior of the friction cone. Since non-marginal equilibrium implies force closure, force closure test can be asserted from whether $P(V\boldsymbol{z}) \succ 0$ has an admissible solution. This inequalities can be solved by a traditional convex optimization technique.

## 7.2 Comparison and Result

For the filtering approach, an obviously preferable property of a necessary condition that is used as the filtering criteria is a large difference in the computational effort between demanded by the criteria and that demanded by the complete method. The difference is the run time to be saved by the approach when the criteria detects a non force closure grasp.

Another preferable property is high specificity of the test. A specificity is the ratio between the number of grasps not satisfying the condition and the total number of non force closure grasps. A high specificity indicates that a large fraction of non force closure grasps are correctly identified by the filtering criteria, and the computational effort is saved by the difference between that of the criteria and that of the complete method.

Aforementioned speedup is then amplified by the number of actual non force closure grasps being tested. This number varies according to the situation that the condition is integrated into. We provide an empirical comparison in the scenario of force closure grasp identification: given an object described by a set of discrete contact points, the task is to identify all force closure grasps.

The comparison is conducted on the six test objects shown in Figure 13. For each object, 100 contact points are randomly sampled to construct the set of all $C_{100,4}$ four-finger grasps. The contact are sampled using the following scheme. For a polygonal object, we randomly select a facet from the polygon and then a point on the facet is randomly selected by repeatedly selecting a point from a smallest rectangle bounding the facet until a point which lies inside the facet selected. This process is repeated until the desired number of contact points are sampled. The curved object in the experiment is described in parametric form. Hence, the sampling is done in the parametric space.

The friction coefficient is assumed to be $\tan(10°)$. Both methods are implemented in C++ using the convex optimization package *maxdet* [30] and the linear algebra package *LAPACK* [31]. The comparison is run on Pentium 4 3.0GHz with 1GB of memory. The result of the comparison is shown in Table 1. The second and the third column show the actual running time of the method in [24] and the filtered version, respectively. Speedup factor is given in the forth column. The number of force closure grasps is given in the fifth column while the number of false positives of our condition is given in the sixth column. The seventh column gives the specificity of our test.

From our experiment, both methods yield the same solution, i.e., force closure grasps identified by both methods are identical. The time used per query of our condition and of the method of Han *et al.* is approximately 0.0056ms and 3.6783ms. This indicates that, for each true negative solution, a running time is reduced to approxi-
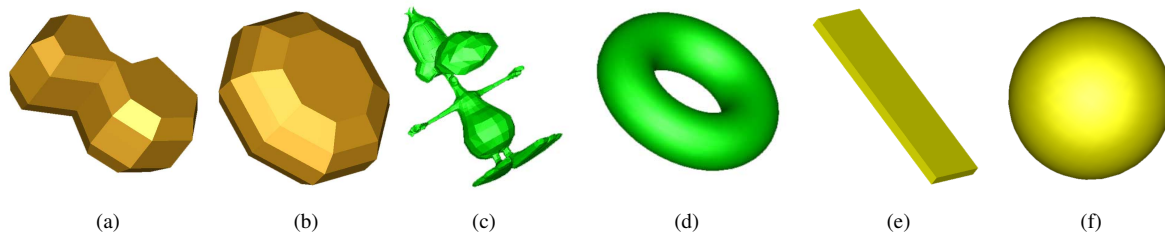
Figure 13: Test Objects.

Table 1: Result of the Experiment

| Objects | Time (seconds) | | | #Solution | #FP | Specificity |
|---|---|---|---|---|---|---|
| | Unfiltered | Filtered | Speedup Factor | | | |
| (a) | 15,486.24 | 709.62 | 21.82 | 253,420 | 110,093 | 0.972 |
| (b) | 15,027.49 | 264.77 | 56.76 | 66,654 | 38,357 | 0.990 |
| (c) | 15,207.18 | 248.24 | 61.26 | 42,366 | 32,450 | 0.991 |
| (d) | 14,969.37 | 269.55 | 55.53 | 193,242 | 39,279 | 0.990 |
| (e) | 14,024.22 | 513.66 | 27.30 | 203,994 | 115,685 | 0.970 |
| (f) | 11,825.03 | 1,041.63 | 11.35 | 916,434 | 635,014 | 0.871 |
| Avg. | 14,423.26 | 507.91 | 39.01 | 279,352 | 161,813 | 0.964 |

mately 0.15%. In the case of false positive, the running time is increased to 100.15%. From the average specificity shown in Table 1, approximately 96.4% of the negative solutions is correctly identified by our condition.

It is clear from the result that our condition exhibits the favorable property of a good filtering criteria. This benefit is more visible when the set of queries contains a large number of non force closure grasps. For example, the circular object (f) has least number of non force closure grasps, i.e., least chance for the filtering criteria to express its benefit and thus the speed up in this case is minimal. On the contrary, the complex object (c) has a large number of non force closure grasps and the speed up in this case is the greatest. Nevertheless, the filtered method using our condition takes one order of magnitude lower running time than the non-filtered version.

# 8   CONCLUSIONS

We have presented a filtering approach for four-finger force closure testing that handles the true quadratic friction cones. The central idea is to apply a necessary condition of force closure to quickly reject non force closure grasps. This condition states that a force closure grasp must be able to generate wrenches that positively span the force space and the torque space independently. An efficient method for testing the condition is developed based on an analysis of the geometric relationship between the friction cones and the force and torque spaces. Specifically, we have presented a simple method to assert whether four force cones positively span the force

space. We have also presented a method to test whether torque sets associated with the force cones positively span the torque space. The method is based on a geometric analysis that the torque set associated with a force cone is either a fan or a plane. An efficiency and effectiveness of our filtering approach has been demonstrated in numerical experiments involving force closure testing of a large number of grasps. The experiment shows that the filtering approach combining our filtering method with a complete method provides much greater efficiency than using a complete method alone.

## Acknowledgment

## REFERENCES

[1] J.K. Salisbury. *Kinematic and force analysis of articulated hands*. PhD thesis, Stanford University, Stanford, CA, 1982.

[2] J.K. Salisbury and B. Roth. Kinematic and force analysis of articulated hands. *ASME J. Mechanisms, Transmissions, and Automation in Design*, 105:33–41, 1982.

[3] A. Bicchi and V. Kumar. Robotic grasping and contact: A review. In *IEEE Int. Conf. on Robotics and Automation*, San Francisco, CA, USA, 2000.

[4] Antonio Bicchi. Hands for dexterous manipulation and robust grasping: A difficult road toward simplicity. *IEEE Trans. Robot. Autom.*, 16(16):652–662, December 2000.

[5] K. B. Shimoga. Robot grasp synthesis algorithms: a survey. *Int. J. Robot. Research*, 15(3):203–266, 1996.

[6] R.C. Brost and K. Goldberg. A complete algorithm for designing planar fixtures using modular components. *IEEE Trans. Robot. Autom.*, 12(1):31–46, February 1996.

[7] Michael Yu Wang. An optimum design for 3-D fixture synthesis in a point set domain. *IEEE Trans. Robot. Autom.*, 16(6):839–846, December 2000.

[8] Yun-Hui Liu, Miu-Ling Lam, and Dan Ding. A complete and efficient algorithm for searching 3-D form-closure grasps in the discrete domain. *IEEE Trans. Robot.*, 20(5):805–816, October 2004.

[9] Jordi Cornella and Raul Suarez. A new framework for planning three-finger grasps of 2D irregular objects. In *IEEE/RSJ Int. Conf. on Intelligent Robots and Systems*, pages 5688–5694, Beijing, Chaina, October 2006.

[10] Xiangyang Zhu and Han Ding. Computation of force-closure grasps: An iterative algorithm. *IEEE Trans. Robot.*, 22(1):172–179, February 2006.

[11] Tetsuyou Watanabe and Tsuneo Yoshikawa. Grasping optimization using a required external force set. *IEEE Transactions on Autmation Schience and Engineering*, 4(1):52–66, January 2007.

[12] Yasuhisa Hasegawa, Junya Matsuno, and Toshio Fukuda. Regrasping behavior and object transition generated by ep. In *Proceedings of the Congress on Evolutionary Computation*, San Diego, CA, USA, 2000.

[13] Yoshiaki Katada, Mikhail Svinin, Kazuhiro Ohkura, and Kanji Ueda. Stable grasp planning by evolutionary programming. *IEEE Trans. Robot. Autom.*, 48(4):749–756, August 2001.

[14] Ch. Borst, M. Fischer, and G. Hirzinger. Grasping the dice by dicing the grasp. In *IEEE/RSJ Int. Conf. on Intelligent Robots and Systems*, Las Vegas, Nevada, USA, 2003.

[15] Yun-Hui Liu. Computing n-finger force-closure grasps on polygonal objects. In *IEEE Int. Conf. on Robotics and Automation*, Leuven, Belgium, 1998.

[16] Xiangyang Zhu, Han Ding, and Jun Wang. Grasp analysis and synthesis based on a new quantitative measure. *IEEE Trans. Robot. Autom.*, 19(6):942–953, December 2003.

[17] Jae-Sook Cheong and A. Frank van der Stappen. Output-sensitive computation of all form-closure grasps of a semi-algebraic set. In *IEEE Int. Conf. on Robotics and Automation*, Barcelona, Spain, April 2005.

[18] Jae-Sook Cheong, Herman J. Haverkort, and A. Frank van der Stappen. On computing all immobilizing grasps of a simple polygon with few contacts. *Algorithmica*, 44:117–136, 2006.

[19] Jae-Sook Cheong and A. Frank van der Stappen. Computing all form-closure grasps of a rectilinear polyhedron with seven frictionless point fingers,. In *Proc. of the IEEE/RSJ International Conference on Intelligent Robots and Systems*, San Diego, CA, USA, 2007.

[20] J. Ponce and B. Faverjon. On computing three-finger force-closure grasps of polygonal objects. *IEEE Trans. Robot. Autom.*, 11(6):868–881, December 1995.

[21] J. Ponce, A. Sudsang, S. Sullivan, B. Faverjon, J.-D. Boissonnat, and J.-P. Merlet. On computing four-finger equilibrium and force-closure grasps of polyhedral objects. *Int. J. Robot. Research*, 16(1):11–35, February 1997.

[22] Xiangyang Zhu and Jun Wang. Synthesis of force-closure grasps on 3-D objects based on the $q$ distance. *IEEE Trans. Robot. Autom.*, 19(4):669–679, August 2003.

[23] Yun-Hui Liu. Qualitative test and force optimization of 3-D frictional form-closure grasps using linear programming. *IEEE Trans. Robot. Autom.*, 15(1):163–173, February 1999.

[24] Li Han, Jeff C. Trinkle, and Zexiang X. Li. Grasp analysis as linear matrix inequality problems. *IEEE Trans. Robot. Autom.*, 16(6):663–674, December 2000.

[25] H. Hashimoto M. Buss and J. Moore. Dexterous hand grasping force optimization. *IEEE Trans. Robot. Autom.*, 12(3):406–418, 1996.

[26] David E. Stewart. Rigid-body dynamics with friction and impact. *SIAM Review*, 42(1):3–39, March 2000.

[27] Xanthippi Markenscoff, Luqun Ni, and Christos H. Papadimitriou. The geometry of grasping. *Int. J. Robot. Research*, 9(1):61–74, February 1990.

[28] B. Mishra, J.T. Schwartz, and M. Sharir. On the existence and synthesis of multifinger positive grips. *Algorithmica, Special Issue: Robotics*, 2(4):541–558, November 1987.

[29] Dan Ding, Yun-Hui Liu, and Shuguo Wang. Computation of 3-D form-closure grasps. *IEEE Trans. Robot. Autom.*, 17(4):515–522, August 2001.

[30] Shao-Po Wu, Lieven Vandenberghe, and Stephen Boyd. *MAXDET Software for Determinant Maximization Problems User Guide*. Stanford University, alpha version edition, 1996.

[31] E. Anderson, Z. Bai, C. Bischof, S. Blackford, J. Demmel, J. Dongarra, J. Du Croz, A. Greenbaum, S. Hammarling, A. McKenney, and D. Sorensen. *LAPACK Users' Guide*. Society for Industrial and Applied Mathematics, Philadelphia, PA, third edition, 1999.